Formation of the Apical Pole of Epithelial (Madin-Darby Canine Kidney) Cells: Polarity of an Apical Protein Is Independent of Tight Junctions While Segregation of a Basolateral Marker Requires Cell-Cell Interactions

Dora E. Vega-Salas, Pedro J. I. Salas, Doris Gundersen, and Enrique Rodriguez-Boulan

Department of Cell Biology and Anatomy, Cornell University Medical College, New York 10021

Abstract. The time course of development of polarity of an apical (184-kD) and a basolateral (63-kD) plasma membrane protein of Madin-Darby canine kidney cells was followed using semiquantitative immunofluorescence on semithin (~0.5-μm) frozen sections and monoclonal antibody probes. The 184-kD protein became highly polarized to the apical pole within the initial 24 h both in normal medium and in 1–5 μM Ca^{2+}, which results in well-spread, dome-shaped cells, lacking tight junctions and other lateral membrane interactions. In contrast, the basolateral 63-kD membrane protein developed full polarity only after incubation in normal Ca^{2+} concentrations for >72 h, a time much longer than that required for the formation of tight junctions (~18 h) and failed to polarize in 1–5 μM Ca^{2+}. These results demonstrate that intradomain restriction mechanisms independent of tight junctions, such as self-aggregation or specific interactions with the submembrane cytoskeleton, participate in the regionalization of at least some epithelial plasma membrane proteins. The full operation of these mechanisms depends on the presence of normal cell-cell interactions in the case of the basolateral 63-kD antigen but not in the case of the apical 184-kD protein.

SECRETORY and transporting epithelia carry out a variety of vectorial functions that depend on the polarization of the plasma membrane into apical and basolateral domains (52, 59). Tight or occluding junctions, located at the boundary between basolateral and apical regions (16, 20), confer on the cell layer the property of a selective barrier to the diffusion of ions and macromolecules (42) and appear to play a role in keeping molecules from both domains segregated (10). Recent work has shown that tight junctions constitute a fence for the movement of lipids in the outer leaflet in the bilayer but not for those in the inner leaflet (11, 68).

A passive fence, however, can maintain but not generate polarity. Other mechanisms have to be postulated to perform this task. In confluent monolayers, with well-developed apical and basolateral poles separated by tight junctions, intracellular sorting mechanisms operating at the level of the Golgi apparatus, have been shown to participate in a vectorial delivery of apical and basolateral proteins to the respective surface domain (4, 37, 39, 46, 51). However, epithelial cells can also generate their surface polarity (and therefore their apical and basal poles) *de novo*. A typical example in vitro is the passage from a round cell suspension to an asymmetric monolayer after trypsinization and replating (6). There are also examples in vivo; perhaps the most striking is the generation of tubule cells from mesenchymal cells during kidney development (15). It is clear that specific cell-substrate and cell-cell interactions must play a crucial role in these cases. In fact, a previous study has shown that junction-free subconfluent epithelial cells, attached to a collagen substrate, can sustain asymmetric virus budding, a polarity property of confluent monolayers (54, 56). However, there is no molecular information on how interaction with the substrate or other cells, which is accompanied, presumably, by basal polarization of receptors for substrate molecules or lateral polarization of cell adhesion molecules (CAMs), leads to the formation of an apical epithelial pole. There is no information either on which are the first apical proteins that are restricted to this apical pole, or on how the tight junctional fence and specific cytoskeletal interactions participate in this process.

Epithelial cell lines are convenient tools to carry out studies of polarization mechanisms (52, 59). The best characterized is the Madin-Darby canine kidney line (MDCK) (35), which preserves the ability of the parental epithelium to generate complete tight junctions and transmonolayer transport of fluid and electrolytes (6, 32, 40). Its structural and functional polarity is evidenced by the asymmetric distribution of enzymes such as aminopeptidase and Na-K ATPase (5, 31, 34, 50), other membrane proteins (1, 25) and intramembrane particles (5, 26), and the polarized budding of enveloped RNA viruses from the cell surface (52, 55, 56, 60).

In this work we followed the development of polarity of

two MDCK cellular membrane proteins, one apical and one basolateral, as a function of the time after attachment to the substrate. We took advantage of the recent observation by Gonzalez-Mariscal and co-workers (19) that MDCK cells plated in 1–5 μM Ca^{2+} form confluent monolayers devoid of tight junctions, but quickly assemble them after Ca^{2+} restoration, to study the role of junctions and cell–cell and cell–substrate contacts in the polarization of apical and basolateral surface markers. The results describe a membrane protein (184 kD) that becomes quickly restricted to the apical pole upon contact with the substrate in the absence of tight junctions; under the same conditions a basolateral marker remains unpolarized.

Materials and Methods

Cells

MDCK cells in the 56th to 70th passage were grown at 37°C in 75-cm^2 disposable plastic bottles (Costar 3150, Cambridge, MA) with an air-5% CO_2 atmosphere at constant humidity in Earle's minimum essential medium (Gibco, Grand Island, NY), supplemented with 100 U/ml of penicillin, 100 μg/ml of streptomycin, and 10% horse serum (complete MEM or cMEM). The cells were harvested with trypsin-EDTA and plated at confluence on plastic ring chambers containing nitrocellulose filters (Millipore Corp., Bedford, MA) coated with rat tail collagen (39, 53). After 90 min at 37°C to allow for cell attachment, the rings were transferred to either fresh cMEM or Ca^{2+}-free MEM (spinner[s] MEM, Gibco), which contains 10 times more phosphate than cMEM and no Ca^{2+}. Calcium levels of this medium were measured by fluorescence assay (66) or by atomic absorption spectroscopy, and found to be 1–5 μM. This concentration is sufficient for cell–substrate attachment (blocked only in the presence of calcium chelating agents) (Salas, P. J. I., D. E. Vega-Salas, and E. Rodriguez-Boulan, unpublished results) but prevents cell–cell interactions and tight junction formation (see Results). Monolayers transferred to sMEM were washed six times at 5-min periods to insure proper removal of Ca^{2+} from the substrate. Controls in cMEM received the same number of washes.

Measurement of the Transepithelial Electrical Resistance

The ring chambers were mounted between two Lucite chambers (the exposed area was 0.78 cm^2) and a continuous current of 20 μA was delivered via Ag/AgCl electrodes. The resulting electrical potential was measured through a second set of electrodes placed at 1 mm from each side of the monolayer. The contribution of the collagen support and the bathing solutions was subtracted (110 ± 22 Ω·cm^2 was mostly due to the bathing solution): all values reported correspond exclusively to the monolayer. A given filter was measured only once and then discarded.

Preparation of Monoclonal Antibodies against MDCK Surface Antigens

BALB/c mice were immunized using confluent MDCK cell monolayers grown on beads (Cytospheres TM, Lux Scientific Corp., Newbury Park, CA). The mice received three biweekly injections; cells fixed with formaldehyde (freshly prepared from paraformaldehyde) and unfixed cells were used alternately to develop high levels of anti-cell surface response.

Hybridoma Production and Screening

The methods for cell fusion and cloning of hybridomas against cell surface antigens have been extensively described (18, 30, 74). Briefly, 0.5–1 × 10^8 NS-1 mouse myeloma cells were fused with preimmunized donor mouse spleen lymphocytes in RPMI 1640 medium, using polyethylene glycol (mol wt 4,000, E. Merck, Rahway, NJ). Cells were plated on spleen macrophage feeder layers in 10 96-well petri dishes in postfusion medium–RPMI 1640 supplemented with 2% HAT: 0.1 mM hypoxantine (Sigma Chemical Co., St. Louis, MO), 0.4 μM aminopterin (Sigma), and 16 μM thymidine (Gibco). After 7–10 d each supernatant was screened for anti-MDCK surface activity by indirect ELISA and immunofluorescence on fixed confluent MDCK monolayers. The immunoglobulin subtypes were characterized in Outcherlony assays using an immunoglobulin subtype identification kit (Boehringer Mannheim Biochemicals, Indianapolis, IN). The apparent molecular weight of MDCK cellular antigens was determined by SDS PAGE of an MDCK detergent extract, followed by electroelution and immunolocalization with monoclonal antibody supernatant, affinity-purified rabbit anti-mouse IgG, and ^{125}I-protein A (65).

Semithin Frozen Sections of MDCK Monolayers

MDCK monolayers were cultivated in cMEM or Ca^{2+}-free MEM on round 12-mm coverslips covered with thin (50–100 μm) native collagen gels. The monolayers were fixed with 2% paraformaldehyde for 1 h, scraped with a razor blade from the coverslip, embedded in 10% gelatin PBS, and infused with 1.8 M sucrose overnight at 4°C. 0.5-μm frozen sections were obtained at −80°C with a Dupont MT-5000 ultramicrotome equipped with the FS1000 frozen sectioning attachment and collected on glass coverslips treated with 1 mg/ml poly-L-lysine. After extensive washing in PBS containing 1% BSA, the sections were processed for indirect immunofluorescence using monoclonal antibodies (67) against cell surface antigens in the first step and affinity-purified rhodamine goat anti-mouse IgG in the second step. After a final short rinse in double-distilled water, the coverslips were inverted and mounted on a drop of 20% Gelvatol (Monsanto Co., Indian Orchard, MA)/15% glycerol in PBS on a glass microscope slide, allowed to harden at room temperature for 2 h, and stored in the cold. Samples were photographed with a Leitz Ortholux epifluorescence microscope (E. Leitz, Rockleigh, NJ) using 400 ASA Kodak Tri-X film (Eastman Kodak Co., Rochester, NY) developed with Diafine for 10 min at 20°C. Exposure time for positive results averaged 20–50 s.

Electron Microscopy

MDCK monolayers on collagen-coated coverslips were fixed with 2% glutaraldehyde in 0.1 M sodium cacodylate buffer at 4°C for 30 min, postfixed with 1% osmium tetroxide in cacodylate buffer, dehydrated in graded ethanols, and embedded in Epon 812. For measurements of tight junction integrity, ruthenium red (5 mg/ml) was included in the osmium step. The correlation between sealed occluding junctions and lack of penetration of various markers has been widely demonstrated (16, 20, 73). Thin sections were mounted on Formvar-coated copper grids, stained with lead citrate, and observed in a JEOL-100X electron microscope (JEOL USA, Peabody, MA).

Stereological Measurements

Apical, basal, and lateral surface areas were measured according to published procedures (22, 70). Average cell volume was estimated from the relationship:

$$V/s = A/b, \quad (1)$$

where V is the average cell volume, s is average area of substrate occupied by a single cell, A is the sectional area of the monolayer, and b is the length of the substrate border in the section. s was measured from the number of cells per surface area unit, as determined by counting nuclei stained with the fluorescent dye Hoechst 33258.

The membrane surface/cell volume density S_v was estimated from the relationship:

$$S_v = 4/\pi\ B/A, \quad (2)$$

where B is the sectional length of the plasma membrane domain under study. The only difference with previously published methods was that both lengths and areas were directly measured using a digital planimeter Microplan II (Laboratory Computer Systems, Inc., Cambridge, MA), rather than using random intersections.

Corrections for Finite Section Thickness. In order to correct S_v values for the bias introduced by finite section thickness t, we used correction factors derived for a model of discrete particles of mean tangent diameter H. Eq. 5 becomes (see reference 71, Eq. 4.19):

$$S_v = 4/\pi\ B'/A' - 4N_a t\ H/(t + H), \quad (3)$$

where B'/A' are apparent border and areas, and N_a is the density number

1. *Abbreviations used in this paper*: cMEM, complete MEM; sMEM, spinner MEM; TER, transmonolayer electrical resistance.

of structures per area. When the particles were considered as whole cells (average values were $N'_a = 7.5 \times 10^{-3}$ μm^{-2}; $t \sim 5 \times 10^{-2}$ μm; H was determined in independent estimates from the number of cells per surface area as 16 μm):

$$4/\pi\ B'/A' \gg 4\ N'_a\ t\ H/(t + H),$$

so that the correction was negligible for the "valleys" between microvilli. For microvilli, however, it was not negligible. The correction factor $K_t(S_v)$,

$$S_v = K_t\ (S_v)\ 4/\pi\ B'/A', \tag{4}$$

was calculated for tubules of diameter d and length L, and only one closed end as shown by Weibel (see reference 71, pp. #118–121 Eqs. 4.58 to 4.66 and 4.89):

$$K_t(S_v) = [r + 1/4]/[r + 1/4 + g\ (1 + 2\ r/\pi)], \tag{5}$$

where $r = L/d$ (ratio length/diameter) and $g = t/d$ (ratio section thickness/diameter). The bias for the microvilli resulted in a 23% correction for S_v in microvilli and ~12% for the entire apical plasma membrane.

Corrections for Anisotropy. A basic assumption for all the estimations in stereology is that the structures are isotropic (randomly oriented in the space). The whole plasma membrane can be considered isotropic. However, because the blocks were oriented so that the section was perpendicular to the substrate, the apical and basal plasma membrane domains resulted parallel and oriented (anisotropic) structures. The bias affected equally apical and basal plasma membrane domains, and caused an overestimation respect to the lateral domain. Two independent attempts to correct this were used: (*a*) Apical and basal apparent border (B') were considered as parallel anisotropic curves in the plane, and estimated by intersections of isotropic lines at angles of 19° and 71° to the substrate orientation (main orientation of both apical and basal membrane domains) as described by Sitte (61; see also reference 71, pp. 291–295). (*b*) A different approach was obtained sectioning MDCK cell monolayers in planes parallel to the substrate. In this case, if $A1$ is the usual longitudinal section (perpendicular to the substrate) and $A2$ is the transverse section (parallel to the substrate) (see reference 71, pp. 299–305, Eq. 10.145):

$$S_v = (4/3\ \pi)\ (B1'/A1' + 2\ B2'/A2'). \tag{6}$$

Both methods corrected an overestimation of the apical and basal with respect to the lateral domain by a factor of 1.6. The values used were obtained by the second method.

The sample sizes were for cells kept in normal calcium: 29 photographs showing 53 cells, and 14 photographs showing 49 cells in the $A2$ section plane. The samples for cells kept in low calcium medium included 18 photographs showing 37 cells and 10 photographs showing 35 cells in the $A2$ section plane.

Microfluorometry

The images from the semithin frozen sections described above were collected directly from the epifluorescence microscope with a silicon intensified SIT 66 video camera (DAGE-MTI, Michigan City, IN), digitized with a PCVISION frame grabber (Imaging Technology, Woburn, MA) and stored in an IBM XT personal computer. Nine images per field were averaged and the result stored for further analysis. Histograms of pixel intensities of each image were performed and only images with pixel values within the linear range were used. Three immunofluorescence intensity profiles per cell, along three different straight lines perpendicular to the monolayer, were collected from each cell image (see Fig. 6). Cell boundaries were avoided because (*a*) 184 kD is mostly excluded in these areas, and (*b*) the complicate geometry of the lateral domain make estimation of membrane densities more complex (see below). The pixel values for apical and basal background (*a* and *e* in Fig. 6) as well as for apical and basal membranes (*b* and *d* in Fig. 6) from each profile were recorded and used to calculate polarity ratios according to the following formulas:

$$\text{Polarity ratio (apical antigen)} = (b - k)F/(d - k); \tag{7}$$

$$\text{Polarity ratio (basal antigen)} = (d - k)/F(b - k), \tag{8}$$

where

$$k = (a + e)/2, \tag{9}$$

and F is a "folding factor" that estimates the amount of folding in the apical and basal membranes, i.e., the presence of microvilli and basal folds, determined using morphometric procedures at the electron microscope level in parallel samples from each experimental condition. Typically, this value was 1.4 in monolayers kept in 1–5 μM Ca^{2+} and 1.51 in monolayers formed in normal medium.

Estimation of the Folding Factor F

The microfluorometric procedure described above is a semiquantitative method to measure the surface polarization of a given antigen. It provides a ratio between the fluorescence intensity per pixel area of apical and basolateral surfaces. In order to correct the measured fluorescence ratios for the "membrane density" in the pixel area (0.31 × 0.23 μm at ×630), it was necessary to estimate the contribution of microvilli and basal folds. Because this is not possible at the optical microscope level (in the same semithin frozen sections), we used morphometric procedures at the EM level. Although these values are obtained in thinner sections of samples fixed and processed differently, the corrections applied are constant for all samples and variations in the ratios for given antigens yield significant estimates of changes in their surface polarization.

Two assumptions were used: (*a*) that the density of membranes under the spot is proportional to S_v, and (*b*) that fluorescence is only in the plasma membrane. The first assumption was justified because semithin frozen sections are ~0.5 μm thick, that is, ~10 times thicker than Epon sections and five times thicker than single microvilli; therefore, each spot is measuring a volume, rather than a two-dimensional section. The second assumption is generally acceptable for plasma membrane proteins, although some intracellular fluorescence may be given by recycling or newly synthesized antigen in precursor pools. As will be discussed in Results, this was particularly true for the measurements of 184 kD in the basal domain during the first day after plating.

Values of B'/A' were calculated by superimposing two parallel lines on EM photographs of sections on the $A1$ plane. The lines were roughly perpendicular to the apical and basal domains, simulating the sections of the fluorescence profile obtained from the digitized images (see Fig. 6). The distance between the lines d' was calculated for each enlargement factor E so that:

$$d' = E\ 0.31\ \mu\text{m}. \tag{10}$$

Then, S_v values were calculated as described before (Eqs. 3–5), except for the correction for anisotropy, that equally affected apical and basal membranes and cancels in Eq. 11. F was calculated as:

$$F = S_v\text{apical}/S_v\text{basal}. \tag{11}$$

Table I. Area of Apical, Lateral, and Basal Membranes in MDCK Monolayers Kept for 20 h in 1–5 μM Ca^{2+} and after Replacement of 1.8 mM Ca^{2+} for 2 h

	1-5 μM Ca (20 h)	1-5 μM Ca → 1.8 mM Ca (2h)
Surface area (domain) (μm^2)		
Apical	2,130 ± 784 (53)	1,490 ± 445 (37)
Lateral	593 ± 783 (53)	3,317 ± 1,322 (37)
Basal	983 ± 194 (53)	875 ± 430 (37)
Total	3,706	5,683
Cell volume (μm^3)	5,167 ± 1,779 (53)	7,146 ± 809 (37)

Confluent MDCK monolayers were plated on collagen-coated nitrocellulose filters and kept in 1–5 μM Ca^{2+} for 20 h. At this time, a group of monolayers (right column) was transferred to medium containing 1.8 mM Ca^{2+} for 2 h. Monolayers were fixed, processed for EM, and their surface areas were measured as described in Materials and Methods. Results are expressed as mean ± standard deviation (number of cells).

Because 184 kD is excluded from cell boundaries (see below), the fluorescence profiles were taken avoiding these areas. So were the measurements of B'/A' for the estimation of F. This introduced a slight difference between F and the ratio S_v apical/basal in the values obtained from the whole apical and basal domains (Table I). This difference was mainly due to the heterogeneous distribution of microvilli and the peculiar geometry of the apical domain in cells kept in low Ca^{2+} medium.

Accuracy of the Microfluorometry Method

To estimate the accuracy of the microfluorometry method for determination of polarity, we used the fact that the apical 184-kD antigen, recognized by the monoclonal antibody S2/2G1 (apical), is mostly excluded from cell–cell boundaries of the apical domain (see Fig. 4 *A*). The ratio of 184-kD antigen density between central and boundary regions of the apical surface, obtained by semiquantitative immunofluorescence, was compared with the ratio obtained by an immunogold procedure and morphometric procedures derived from those used by Griffiths et al. (21). Confluent MDCK cell monolayers grown in normal calcium medium for 24 h were fixed in 2% paraformaldehyde/0.1% glutaraldehyde, treated sequentially with S2/2G1 monoclonal antibody, affinity-purified anti-mouse rabbit IgG, and colloidal gold coupled to protein A, postfixed with 2% glutaraldehyde and processed for EM. The gold particle ratio between central regions and the peripheral 1 μm of the apical plasma membrane domain, determined on 17 cells, was 0.25, which compared well with the ratio obtained with the video enhancement procedure (0.22).

Statistics

Normal distribution was tested for "goodness-of-fit" through the χ^2 test and used for all the variables. Unless otherwise stated, the values are given as mean ± standard deviation (number of cases). For stereologic measurements, corresponding equations and corrections were used on a cell-by-cell basis, and standard deviation formulas were applied to sets of final estimations of membrane surfaces. Significance of differences between mean values was assayed by Student's *t* test.

Results

Calcium Dependence of the Sealing of Occluding Junctions

When MDCK cells, dissociated by trypsin-EDTA treatment, are plated in normal medium (cMEM, contains 1.8 mM Ca^{2+}) at high density on collagen-coated nitrocellulose filters, they form a continuous monolayer in ~60–90 min. If incubation in normal medium is continued, a transmonolayer electrical resistance (TER) starts to develop in ~4 h and reaches a maximum in 15–20 h (6). Monolayers that are switched to 1–5 μM Ca^{2+} (sMEM containing no chelators) after 90 min of plating in MEM do not develop any TER in 20 h; if they are transferred to cMEM at this point, normal levels of TER are reached in only 4 h in a process independent of protein synthesis (19). To determine the minimum Ca^{2+} levels required to form tight junctions, MDCK cells were plated in cMEM for 90 min and then transferred to media containing various levels of Ca^{2+} for 24 or 72 h (Fig. 1). Maximum levels of resistance were observed with Ca^{2+} concentrations above 0.1 mM, 18 times smaller than the Ca^{2+} levels in the normal medium. Half-maximum values of TER were observed at ~50 μM Ca^{2+}. Similar Ca^{2+} dependence functions were observed after 24 or 72 h of plating.

Structure of MDCK Monolayers Developed in Ca^{2+}-free Medium

Examination under the electron microscope of MDCK monolayers kept for 20 h in 1–5 μM Ca^{2+} showed that cells maintained under these conditions had a strikingly altered morphology: they were dome-shaped, with most of the microvilli concentrated in the bulging center and an almost absent lateral plasma membrane surface (Fig. 2 *A*). Quantitative morphometry experiments (Table I) showed that the lateral surface (defined as the membrane area limited by the substrate and the cell–cell contact closest to the free surface) constituted only 16% of the total cell surface area. Restoration of 1.8 mM Ca^{2+} for just 2 h resulted in an increase of the lateral surface area to normal values of 58% of the total cell surface area (Fig. 2 *B*, Table I), with the apical area decreasing slightly and the basal surface remaining relatively unchanged. Thus, the formation of the lateral surface after Ca^{2+} replacement probably requires the addition of new membrane to the cell surface and involves a 38% increase in cell volume. The mechanisms underlying these changes remain to be investigated. Parallel determinations with ruthenium red in the same monolayers showed that, from all cell pairs examined in the monolayers formed in Ca^{2+}-free medium, 57% showed no lateral surfaces, 30% had lateral surfaces accessible to ruthenium red, and only 13% had inaccessible lateral membranes. After 2 h in 1.8 mM Ca^{2+} (see also Fig. 2 *B*), 58% of the cell pairs exhibited functional occluding junctions and all cells had well-developed lateral surfaces.

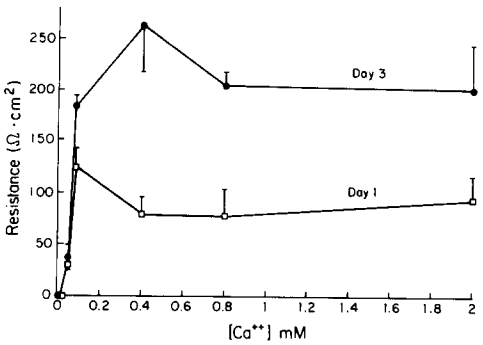

Figure 1. Effect of calcium on the development of tight junctions. MDCK cells were plated at immediate confluency on collagen-coated nitrocellulose filters bound to plastic rings. After 90 min in cMEM 10% FCS, to allow attachment to the substrate, the cells were transferred to MEM containing various calcium concentrations. TER was determined in seven independent measurements, 1 and 3 d after plating. In both cases the Ca^{2+} concentration giving half-maximum effect is ~50 μM.

Surface Distribution of Intrinsic Apical and Basolateral Surface Proteins in MDCK Monolayers Kept in Micromolar Calcium

To study the effect of disrupting tight junctions and cell–cell interactions on the distribution of intrinsic MDCK surface markers, we carried out studies with two monoclonal antibodies developed in our laboratory (67), which recognize apical (hybridoma S2/2G1) and basolateral (hybridoma S2/3G2) surface antigens of MDCK cells (see Fig. 4). These antigens are membrane proteins with SDS PAGE mobilities of, respectively, 184 and 63 kD, as detected by immunoblot (Fig. 3); the epitopes recognized by the monoclonals are not carbohydrate residues because treatment with periodate does not decrease the affinity for the monoclonal antibody (data

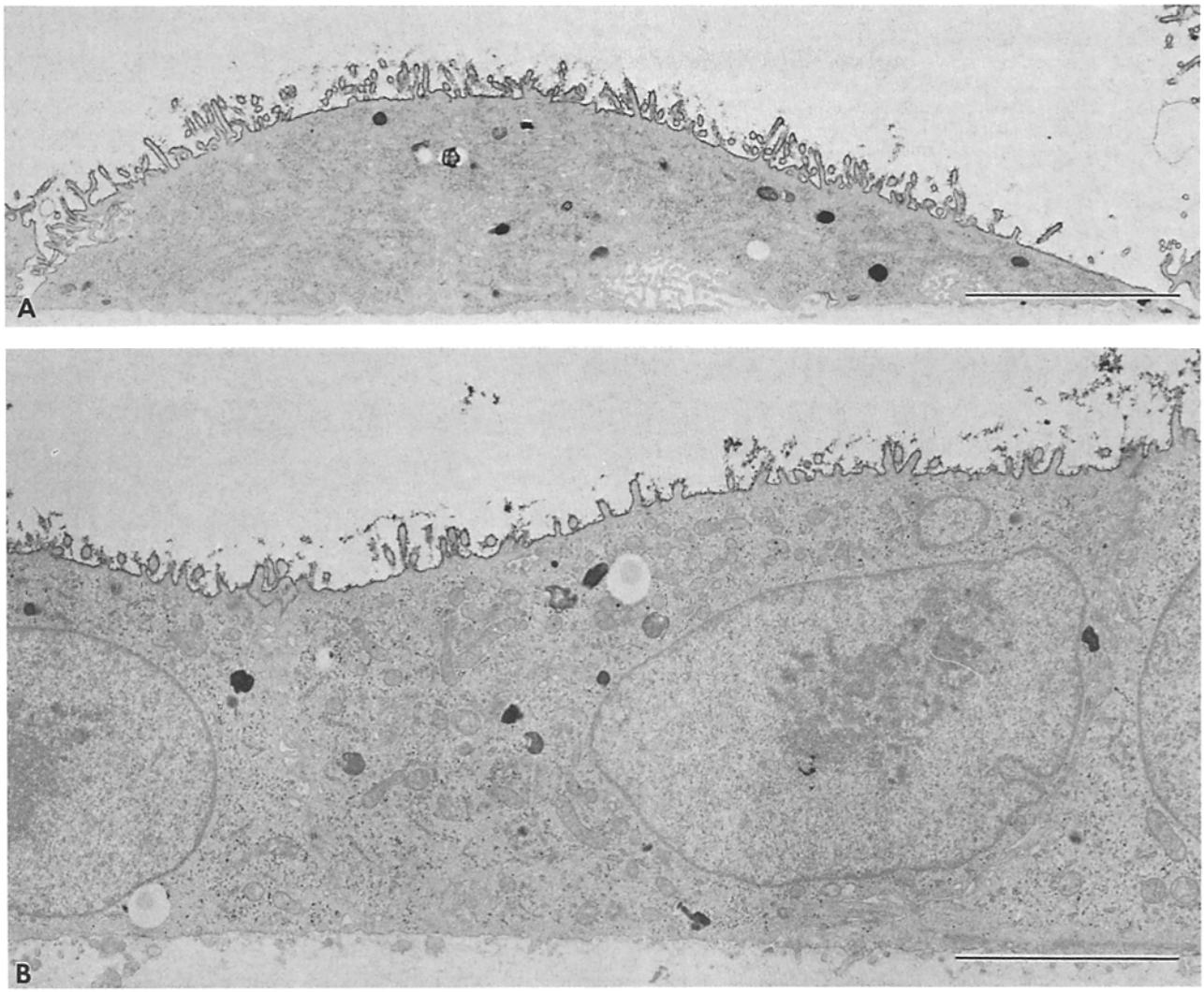

Figure 2. Structure of MDCK cells maintained in 1–5 μM Ca^{2+}. MDCK cells were plated on collagen gels at immediate confluency in cMEM. After 90 min the medium was replaced by sMEM (containing 1–5 μM Ca^{2+}) and the monolayers were incubated overnight. After 20 h in culture, the concentration of Ca^{2+} in one set of monolayers (*B*) was raised to 1.8 mM while the other set (*A*) was kept in 1–5 μM Ca^{2+}. The monolayers were fixed 2 h later in 2% glutaraldehyde, postfixed with osmium tetroxide (containing ruthenium red), and processed for EM. Cells in 1–5 μM Ca^{2+} have a dome-shaped appearance and almost no lateral surface. After Ca^{2+} replacement for 2 h, the lateral surface has developed and many junctions become impermeable to ruthenium red. Bars: (*A*) 3.8 μm; (*B*) 3.6 μm.

not shown). Interestingly, the apical antigen behaves differently from influenza hemagglutinin or other apical antigens of MDCK cells in that it is excluded from peripheral (boundary) regions of this surface (Fig. 4 *A*).

Immunofluorescence on semithin (0.5 μm) frozen sections showed that, in MDCK monolayers kept in 1–5 μM Ca^{2+} for 20 h, the apical 184-kD antigen was strikingly polarized to the free surface (Fig. 5, *A* and *B*). Again, in this case, this protein appeared to be concentrated in the center of the free surface (Fig. 5 *A*). On the other hand, the basolateral 63-kD antigen was found to be distributed over both the free and the attached surface (Fig. 5, *C* and *D*), in agreement with previous results with basolateral antigens by Herzlinger and Ojakian (25) and Balcarova-Stander et al. (1). Furthermore, after 2 h of Ca^{2+} replacement, when 58% of the tight junctions were already functional (Table I), as detected by lack of penetration of ruthenium red, the 63-kD antigen was still unpolarized (Fig. 5, *E* and *F*).

Kinetics of Polarization of the 184- and 63-kD Proteins

To follow the kinetics of polarization of both surface markers under various experimental conditions the immunofluorescence images obtained from the semithin frozen sections were collected from the epifluorescence microscope with a video camera and digitized. To decrease the image noise, nine images of the same field were averaged and the resulting image was stored in the computer hard disk for analysis of polarity. Photographs of typical stored images of monolayers stained with the 184- and the 63-kD monoclonal antibodies, taken directly from the video monitor screen, are shown in Fig. 6 (*lower panels of each pair*). For each monolayer, the fluorescence intensity profile along a perpendicular line is shown in the corresponding upper panel. Because all the points (pixels) were kept automatically within the linear range of the camera (see Materials and Methods), this proce-

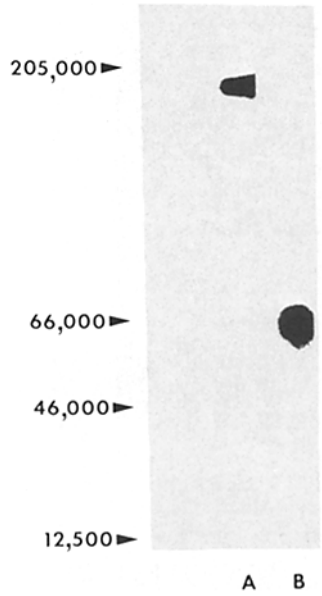

Figure 3. Immunoblot of MDCK proteins carrying epitopes for monoclonal antibodies raised against the cell surface. Postnuclear supernatants of MDCK monolayers scraped in the presence of 1 mM EDTA, 0.4% Nonidet P-40, and 0.1% DOC were processed for SDS PAGE and electroeluted on nitrocellulose filters. The filters were cut longitudinally in 1-cm-wide strips. Each strip was exposed to one hybridoma supernatant, affinity-purified rabbit anti-mouse IgG and ^{125}I-protein A, washed, dried, and exposed to X-ray film. Apparent molecular mass of the antigens (184 kD and 63 kD) was obtained by comparison with protein standards stained with amido black. The autoradiogram is shown for (*A*) hybridoma S2/2G1 (anti-apical membrane protein) and (*B*) hybridoma S2/3G2 (anti-basolateral membrane protein).

dure provides a good estimate of the fluorescence ratios between any given pair of points in the image.

Three independent measurements were made for each cell, along three different perpendicular lines, of apical and basal membrane fluorescence (*b* and *d*), apical and basal background fluorescence (*a* and *e*), and cytoplasmic background. The ratio apical/basal membrane fluorescence ("polarity ratio") was calculated after subtracting the average extracellular background from the peak values of fluorescence in the basal and apical membranes. The ratio includes a correction factor for the amount of folding in the apical and basal membranes ("membrane densities"), which accounts for the presence of apical microvilli and basal folds (see Materials and Methods). The polarity ratios thus corrected provide a semiquantitative measure of the apical/basal antigen density ratio between both membranes.

The polarity ratios of the 184- (apical) and the 63-kD (basal) antigens were studied as a function of time after cell plating. Both ratios were approximately 2 at 90 min after plating, when most of the cells had attached and spread on the substrate but showed no morphologic cell–cell interactions. This indicates that a certain degree of polarity developed rapidly upon interaction with the substrate. The 184-kD protein reached 85% of its full polarity (ratios 10–15) in the

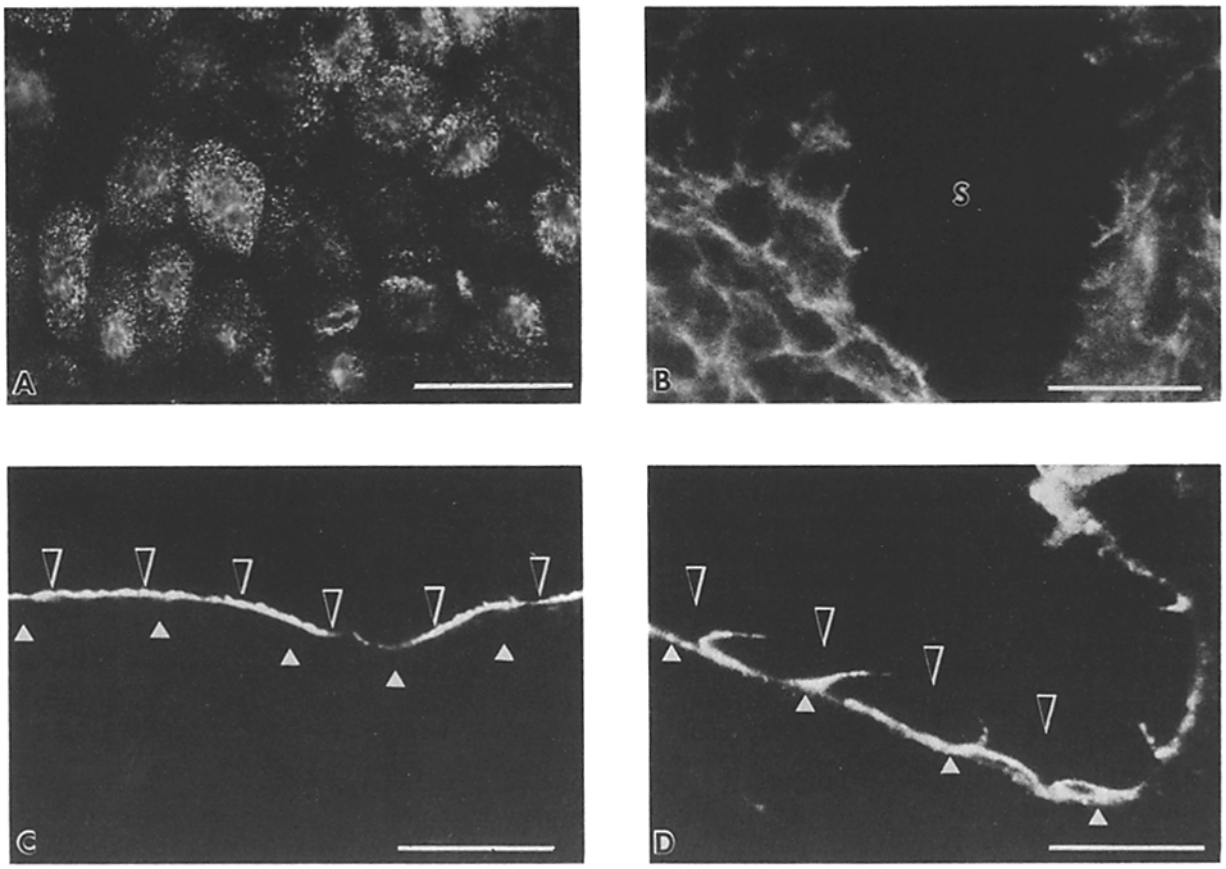

Figure 4. Immunofluorescence of anti-MDCK cell membrane protein monoclonal antibodies. Confluent MDCK cell monolayers were grown on glass coverslips (*A* and *B*) or on collagen gels (*C* and *D*) for 3 d and fixed in 2% paraformaldehyde. Whole monolayers (*A* and *B*) or 0.5-μm frozen sections of them (*C* and *D*) were processed for immunofluorescence using the supernatant of hybridoma S2/2G1 (*A* and *C*) or S2/3G2 (*B* and *D*) in the first step and affinity-purified rhodamine-coupled goat anti-mouse IgG in the second step. In the frozen sections, the large arrowheads indicate apical surface and small arrowheads indicate basal surface. The 184-kD antigen is exclusively apical while the 63-kD antigen is basolateral. In monolayers grown on coverslips (*B*), the 63-kD antigen fluorescence was visible only in the vicinity of a scratch (*S*). Bars: (*A*) 24 μm; (*B*) 30 μm; (*C*) 18 μm; (*D*) 15 μm.

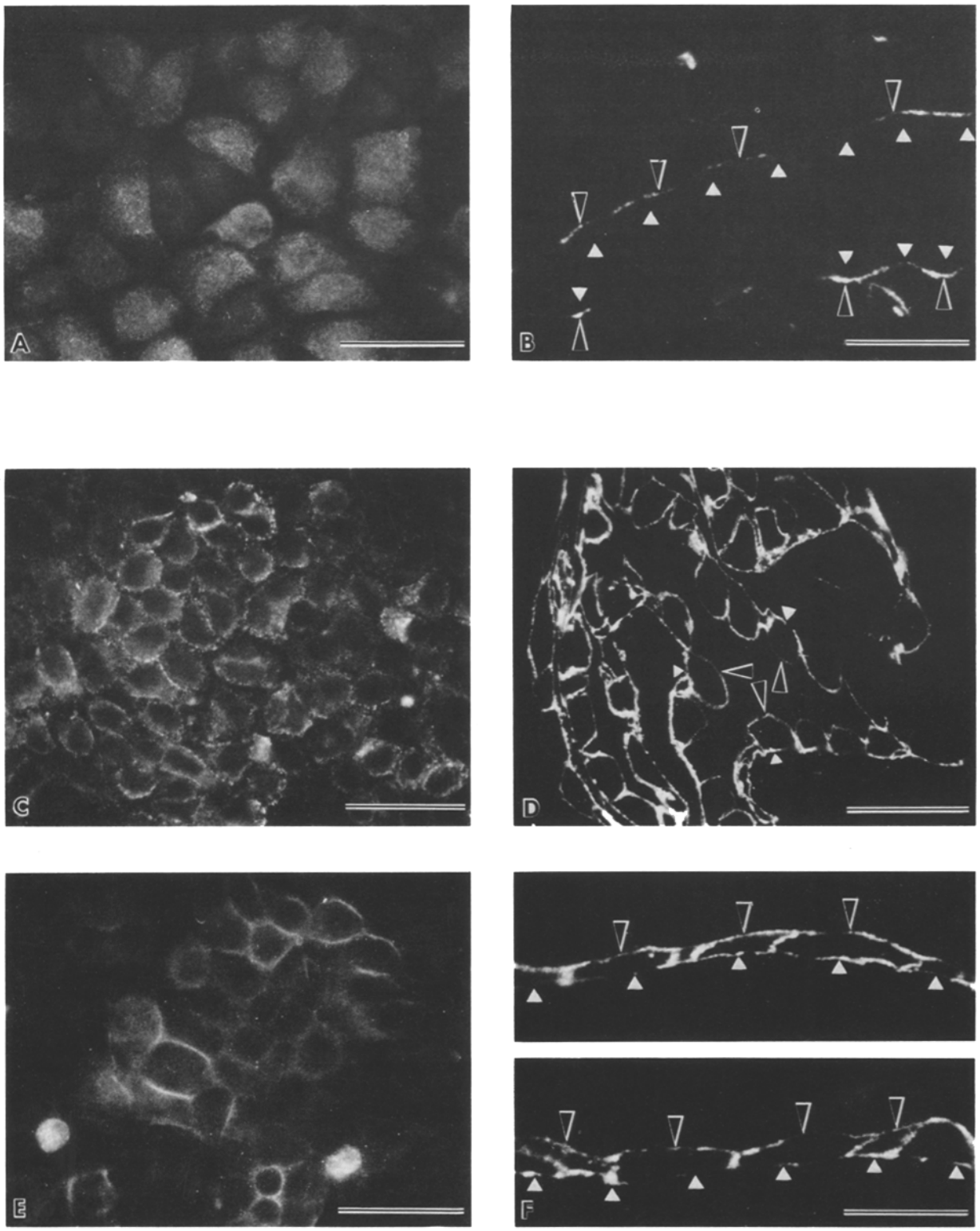

Figure 5. Immunofluorescence localization of apical and basolateral surface antigens in MDCK monolayers grown in micromolar calcium. Confluent MDCK monolayers on glass coverslips (*left panels*) or on collagen gels (*right panels*) were maintained for 20 h in 1–5 Ca^{2+} (*A–D*); monolayers *E* and *F* were transferred to 1.8 mM Ca for an additional 4 h. All cells were fixed in 2% paraformaldehyde; monolayers grown on collagen (*right panels*) were frozen sectioned. Cells on coverslips and frozen sections were processed for indirect immunofluorescence with monoclonal antibodies S2/2G1 (*A* and *B*) (specific for an apical 184-kD antigen) and S2/3G2 (*C–F*) (against a basolateral 63-kD protein). In the frozen sections, the large arrowheads point at the apical surface and small arrowheads point at the basal surface. The frozen sections clearly show that the apical 184-kD protein is polarized in the presence of micromolar calcium (*B*), while the basolateral 63 kD antigen is not (*D*). After 4 h in 1.8 mM calcium the cells form lateral membrane (and functional tight junctions as shown in Fig. 2) but the 63-kD protein is not yet polarized. In intact monolayers the 63-kD basolateral protein is accessible to antibodies added from above (*C* and *E*), differently from what was observed (Fig. 4) in MDCK monolayers confluent for several days. Bars: (*A*, *B*, and *E*) 24 μm; (*C*) 31 μm; (*D*) 26 μm; (*F*) 18 μm.

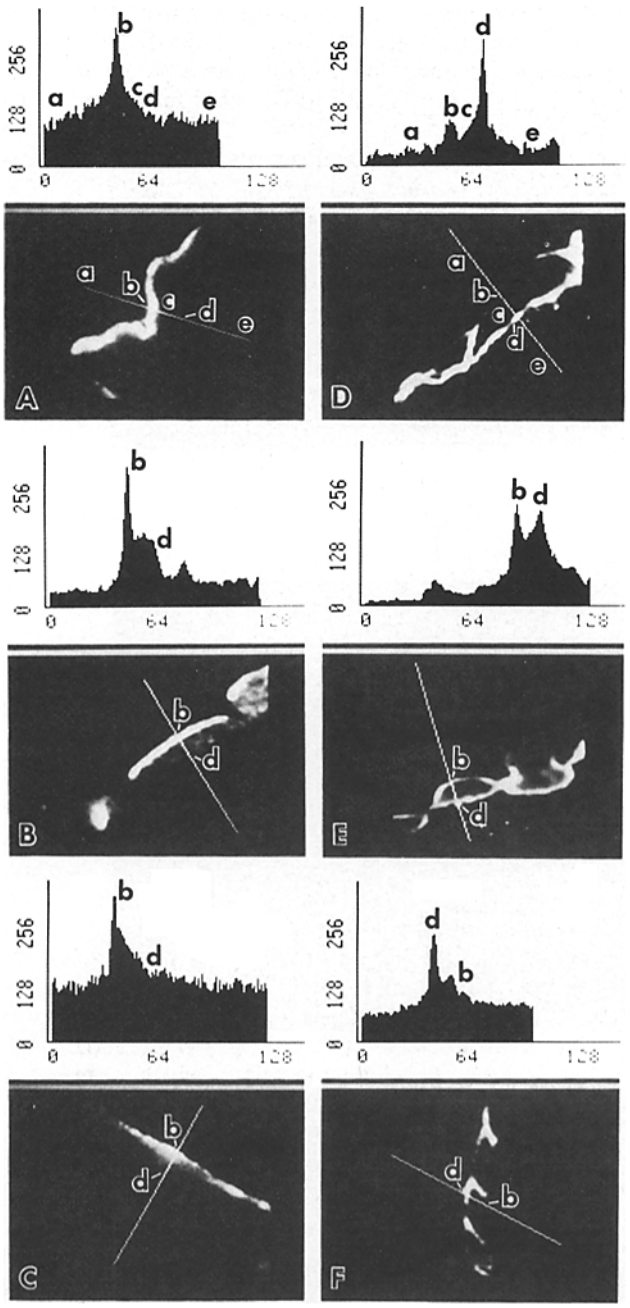

Figure 6. Digitized immunofluorescence profiles of apical and basolateral plasma membrane proteins in semithin frozen sections of MDCK cells. Semithin frozen sections of MDCK cell monolayers were obtained and processed for immunofluorescence as described in Fig. 5. Digitized images were obtained directly from the epifluorescence microscope with a silicon intensified video camera, and stored in the computer. For each pair, the upper panel shows the light intensity profiles (pixel values 0–255) over the straight line traced on the cell image in the lower panel. Typically (see *A* and *D, top panels*), the profiles showed extracellular background levels of 20–70 (*a* and *e*). The exact position of the apical and basal membranes was obtained from the corresponding phase image in each case. Peaks of apical (*b*) and basal membrane (*d*) fluorescence ranged 200–256 in highly positive membranes. Cytoplasmic fluorescence (*c*) levels ranged over 50–150. Typical profiles are shown for cells: (*A*) confluent for 24 h in normal calcium medium, apical antigen; (*B*) kept in low calcium medium for 24 h, apical antigen; (*C*) kept in low calcium medium for 24 h and then transferred to normal calcium medium for an additional 24 h, apical antigen; (*D*) kept in normal calcium medium for 72 h, basolateral antigen; (*E*) kept in low calcium medium for 72 h, basolateral antigen; and (*F*) kept in low calcium medium for 48 h and transferred to normal calcium for an additional 24 h, basolateral antigen. Note that the fluorescence levels of the apical antigen in the basal membrane (*d*) are not significantly higher than cytoplasmic fluorescence levels, while basolateral antigen levels in the apical membrane are always higher than cytoplasmic fluorescence levels.

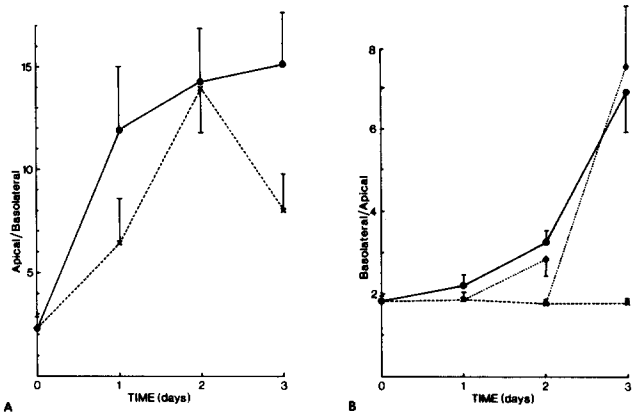

Figure 7. Polarity ratios of apical and basolateral MDCK plasma membrane proteins at various times after plating in normal or low calcium media. Polarity ratios were obtained from the digitized images described in Fig. 6, using three profiles per cell randomly selected. Apical/basal and basal/apical polarity ratios were calculated by subtracting the average extracellular background from the fluorescence in the apical and basal membranes. Each point represents the average of triplicate measurements on 12–32 cells. Polarity ratios are shown as a function of time after plating (time 0 = 90 min after plating) for MDCK cell monolayers in normal calcium medium (*solid circles*), in low calcium medium (×) or kept in low calcium medium for 1 or 2 d and then shifted to normal calcium medium for an additional 24 h (*solid diamonds*).

first 24 h of plating in normal calcium medium (Fig. 7 *A*, *solid circles*). Cells incubated in low calcium medium showed ratios of 6–7 at 24 h and 14–15 at 48 h (Fig. 7 *A*, ×), similar to the ratios of control cells at 48 h. The difference observed at 24 h may actually result from an underestimation of the ratio for the cells in low calcium medium owing to higher cytoplasmic levels of fluorescence at this time (see Fig. 6 *B*). The decrease of the polarity ratio after 72 h in low calcium medium may reflect cell damage in monolayers kept continuously in low calcium medium.

The kinetics of development of polarity of the 63-kD (basolateral) protein were very different from those observed for the 184-kD (apical) protein. In monolayers kept in normal cMEM (Fig. 7 *B*, *solid circles*), the polarity ratio of this protein was 2 (higher in the basal membrane) 90 min after plating, increased slowly during the first 48 h, and then rapidly between the second and third days after plating; polarity ratios jumped from 3 to 7 (Fig. 7 *B*) and reached a maximum of 19 ± 3 during the fourth day (not shown). Parallel radioimmunoassay experiments showed a slow decrease in the amount of basolateral protein located in the apical membrane (the amount at the fourth day was about one-half of the amount after plating, data not shown), suggesting redistribution or removal of the protein by turnover.

A striking difference with the 184-kD antigen was the absolute lack of further polarization in low calcium medium (Fig. 7 *B*, ×). However, cells kept in low calcium medium developed the capability of repolarizing the basolateral antigen upon restoration of calcium to normal concentrations with the same kinetics as control monolayers (Fig. 7 *B*, *solid diamonds*). In fact after replacing Ca^{2+} on the first and the second days, the polarity ratios reached values similar to control monolayers within 24 h.

Discussion

Formation of the Apical Pole of MDCK Cells upon Cell Attachment to the Substrate

Our observations describe for the first time an apical epithelial membrane protein of 184 kD that fully polarizes in the absence of cell–cell interactions and tight junctions, just upon attachment of the cells to the substrate. This protein reached full polarity levels within the first 24–48 h both in monolayers formed in 1.8 mM Ca^{2+}, which have complete tight junctions (6), and in monolayers developed in 1–5 μM Ca^{2+}, which lack functional tight junctions. Presumably, a class of other apical components will be identified that shares this property. The "capping" of the 184-kD protein on the pole opposite to the attached surface is reminiscent of the polarization of concanavalin A receptors to form an apical pole during the compaction stage of egg development (29, 75), although in the latter case it was not explored whether it was caused by an increased number of microvilli or increased antigen density in the membrane.

The results presented here complement and expand our previous report that, in subconfluent MDCK monolayers lacking extensive cell–cell interactions and tight junctions, virus budding is polarized (54). Thus, the putative apical components involved in apical budding of influenza must belong to the same class of proteins as the 184-kD marker. Future work is necessary to determine how general is the polarization of apical proteins in response to substrate attachment.

Mechanism of Repolarization of Basolateral Proteins

Differently from the 184-kD marker, the basolateral 63-kD protein maintained initial low levels of polarity (approximately two times) during the first 48 h of incubation in normal Ca^{2+}, even when tight junctions develop in 18 h (19), but became quickly polarized during the third and fourth days. In 1–5 μM Ca^{2+}, 63 kD was practically unpolarized for up to 72 h (longer times could not be studied because the cells rapidly lost viability after this time). Restoration of normal Ca^{2+} levels for 24 h to monolayers kept in 1–5 μM Ca^{2+} resulted in low polarity values when carried out during the second day, but in full polarization of the 63-kD protein during the third day (Fig. 7 *B*), even when in both cases tight junctions formed in ~4 h (Table I). These results indicate that an internal "clock," acting both in the absence or in the presence of Ca^{2+}, regulates the development of the mechanism involved in the polarization of the basolateral marker. This mechanism is fully developed 48 h after dissociation; however, its function (detected as full polarization of the 63-kD protein) requires the presence of Ca^{2+} and, presumably, of normal cell–cell interactions. Na-K ATPase, another basolateral marker, also may require 3 d to repolarize fully after cell dissociation (62; D. Gundersen and E. Rodriguez-Boulan, unpublished results) and, thus, probably uses the same mechanism. We have no information on the nature of this mechanism. Misplaced 63-kD protein may be relocated by vesicular transcytosis, as described for the translocation of exogenous vesicular stomatitis virus (VSV) G protein implanted by viral fusion into the apical membrane of MDCK cells to the basolateral surface (36, 45), or may be degraded and polarity may be established by vectorial insertion of newly synthesized protein in the correct domain. Perhaps these mechanisms require 2–3 d to become fully effective. Alternatively, the delay in the acquisition of polarity of the 63-kD marker may reflect the time necessary for the synthesis and accumulation of critical levels of putative cellular or extracellular molecules required for polarization of basolateral proteins, such as basement membrane glycoproteins, uvomorulin-like cell adhesion molecules, or components of the submembrane cytoskeleton (see below).

The Fence Role of Tight Junctions

Our observations indicate that tight junctions are not necessary for the polarization of the apical 184-kD protein and may be not sufficient for the polarization of the basolateral 63-kD marker. Thus, they challenge the notion that the tight junctional fence is an absolute requirement for the maintenance of epithelial cell surface segregation. In fact, when carefully examined, the evidence for this notion is largely circumstantial. Removal of Ca^{2+} by chelating agents results in the opening of occluding junctions and the invasion of the apical and basolateral regions by markers previously segregated (25, 47, 75). However, it may be argued that the chelating agents may be simultaneously affecting an independent polarization mechanism. Intramembrane particles (17, 58, 64), normally present at higher densities in the basolateral surface of MDCK cells (5, 9, 26) become depolarized in monolayers formed in 1–5 μM Ca^{2+} (19) and polarize with the same kinetics as occluding junctions, which is prevented by inhibitors of tight junction formation, e.g., cycloheximide or cytochalasin B (26). As in the previous case, independent surface polarization mechanisms might be affected simultaneously with the tight junctions by these treatments. It has been reported (1, 25) that basolateral antigens are present in relatively high levels in the apical surface of subconfluent epithelial monolayers, which lack complete tight junctions; these studies, however, did not quantitate surface polarity and were not accompanied by corresponding observations on the behavior of apical proteins with procedures that allow simultaneous examination of free and attached membrane regions.

Role of the Substrate in Polarity

The observation that both 184- and 63-kD antigens become polarized after attachment to the substrate, even at times as short as 90 min (studied for the nonviral antigens, Fig. 7) highlights the organizational role of the substrate in the development and maintenance of epithelial polarity. It is possible that the low level of polarity observed 90 min after attachment (approximately two times, Fig. 7) reflects the recruitment of substrate receptors and the consequent coenrichment of basolateral markers and exclusion of apical markers. A good example of this process is the recruitment of macro-

phage Fc receptors on an immunoglobulin-coated surface and the consequent depletion of receptors from the free surface (38).

Substrate attachment has been shown to play an important role in the development of epithelial cell polarity in other systems. Thyroid cells in culture reverse their polarity after addition of a collagen substrate to the apical surface (7, 44); some cell lines develop a lumen when surrounded with collagen (24) whereas MDCK cells redistribute an apical membrane protein when cultured within collagen gels (67a). Of particular relevance to our studies is the observation by Ingber et al. (28) that pancreatic tumor epithelial cells, unable to synthesize their own basement membrane components, polarize their intracellular organelles when plated on laminin but not on type I collagen. Recently described receptors for collagen (63, 69; Salas, Vega-Salas, and Rodriguez-Boulan, manuscript in preparation) or basal lamina components, such as laminin (33), are excellent candidates to play a critical role in these processes.

Cell–Cell Interactions and Epithelial Polarity

In addition to tight junctions, several other cell–cell interactions are present at the level of the lateral surface. Adherent junctions, desmosomes, and gap junctions are all dependent on the presence of Ca^{2+} to various extents. L-CAM and uvomorulin-like molecules play an additional role in epithelial cell recognition and adhesion (13, 14, 23, 27); at least some of these molecules are also dependent on Ca^{2+}. Thus, the formation of the lateral surface is the result of various adhesive forces, with a spectrum of Ca^{2+} sensitivities (13). Our experiments indicate that the mechanisms involved in attachment to the substrate have a considerably lower requirement for Ca^{2+} than those involved in the formation of the lateral surface. MDCK cells kept in 1–5 μM Ca^{2+} have a dome-shaped, "contracted" appearance, with a very reduced lateral surface, similar to the morphology of mammary epithelial cells briefly treated with EGTA described by Pitelka et al. (48, 49). Our results also show that the minimum Ca^{2+} concentration required for the sealing of occluding junctions is 50–100 μM (18 times lower than the concentration of Ca^{2+} in the normal medium).

That cell–cell interactions play a role in the development and maintenance of epithelial cell polarity is clearly demonstrated by the previous observation that clumps of MDCK cells in suspension culture (lacking cell–substrate interactions) show polarized budding of viruses (54). Interestingly, MDCK cells treated with chelating agents (25, see Introduction) lose their surface polarity. Experimental dissection of cell–cell from cell–substrate interactions by incubation of the MDCK monolayers in 1–5 μM Ca^{2+} allowed us to obtain important new information on how each type of interaction contributes to the polarization of apical and basolateral markers. The experiments described in this report clearly implicate cell–cell interactions in the polarization of the basolateral 63-kD protein.

Role of the Submembrane Cytoskeleton in Epithelial Polarity

In addition to the evidence discussed above, recent work from other laboratories suggests a role for the submembrane cytoskeleton in epithelial polarity. This structure has been best characterized in the erythrocyte by the work of Branton, Bennett, and their colleagues (see references 2 and 3 for reviews). Recent reports demonstrate that the erythrocyte's anion channel band 3 is present in kidney epithelial cells, where it is restricted to the basolateral surface (12). Two polypeptides, ankyrin and spectrin, which in erythrocytes form a submembrane fibrous network that anchors band 3 (8), are restricted to the same surface domain (12) of kidney cells. In MDCK cells, a highly insoluble, relatively dense layer of spectrin, apparently localized to the basolateral surface of MDCK cells, develops with the same kinetics as the polarization of Na-K ATPase (43).

Thus, a possible interpretation of the delayed polarization of the 63-kD (basolateral) marker is that cell dissociation disrupts the ankyrin–spectrin system and that an incubation of 48 h is needed for its reconstitution. Analogously, a variety of proteins underlying the apical surface are good candidates to fulfill such a role for the apical surface (41). Cytochalasin-sensitive actin filaments and tubulin, though, do not seem to be critically involved in the maintenance of epithelial polarity (57) and do not appear to participate in the reorganization of the basolateral spectrin network during reformation of MDCK monolayers. Future work should attempt to identify specific interactions between cytoskeletal and membrane components that may participate in the polarization of apical and basolateral proteins in epithelial cells.

We thank Drs. Donald Fischman and Doris Wall for critically reading the manuscript; Dr. Fred Maxfield, New York University, for advice with microfluorometry and video analysis; Drs. Connie Finstad and Rosemarie Ramsewak, Memorial Sloan-Kettering Cancer Center, for their help and advice with the hybridoma technology; Dr. Brenda Eisenberg, for advice on morphometric proceedings; and Ms. Maria Perez and Mr. Wayne Fries for the electron microscopy.

This work was supported by research grants from the National Institutes of Health (GM-34107), National Science Foundation (DCB-8442489 and INT-841440), American Heart Association, New York Branch, by an International Fogarty fellowship to Dr. Salas and by an Irma T. Hirschl research career award and an Established Investigator award from the American Heart Association to Dr. Rodriguez-Boulan.

Received for publication 23 September 1986, and in revised form 10 November 1986.

References

1. Balcarova-Stander, J., S. E. Pffeiffer, S. D. Fuller, and K. Simons. 1984. Development of cell surface polarity in the epithelial Madin-Darby canine kidney (MDCK) cell line. *EMBO (Eur. Mol. Biol. Organ.) J.* 3:2687–2694.
2. Bennett, V. 1982. The molecular basis for membrane- cytoskeleton association in human erythrocytes. *J. Cell. Biochem.* 18:49–65.
3. Branton, D., C. Cohen, and J. Tyler. 1981. Interaction of cytoskeletal proteins on the human erythrocyte membrane. *Cell.* 24:24–32.
4. Caplan, M. J., H. C. Anderson, G. E. Palade, and J. D. Jamieson. 1986. Intracellular sorting and polarized cell surface delivery of (Na^+,K^+) ATPase, an endogenous component of MDCK cell basolateral plasma membranes. *Cell.* 46:623–631.
5. Cereijido, M., J. Ehrenfeld, I. Meza, and A. Martinez-Palomo. 1980. Structural and functional membrane polarity in cultured monolayers of MDCK cells. *J. Membr. Biol.* 52:147–159.
6. Cereijido, M., E. S. Robbins, W. J. Dolan, C. A. Rotunno, and D. D. Sabatini. 1978. Polarized monolayers formed by epithelial cells on a permeable and translucent support. *J. Cell Biol.* 77:853–880.
7. Chambard, M., J. Gabrion, and J. Mauchamp. 1981. Influence of collagen gel on the orientation of epithelial cell polarity: follicle formation from isolated thyroid cells and from preformed monolayers. *J. Cell Biol.* 91:157–166.
8. Cox, J. V., R. T. Moon, and E. Lazarides. 1985. Anion transporter: highly cell-type specific expression of distinct polypeptides and transcripts in erythroid and non erythroid cells. *J. Cell Biol.* 100:1548–1557.

9. DeCamilli, P., D. Peluchetti, and J. Meldolesi. 1974. Structural differences between luminal and lateral plasmalemma in pancreatic acinar cells. *Nature (Lond.).* 248:245–246.
10. Diamond, J. M. 1977. The epithelial junction: bridge, gate and fence. *Physiologist.* 20:10–18.
11. Dragsten, P. R., J. S. Handler, and R. Blumenthal. 1982. Fluorescent membrane probes and the mechanism of maintenance of cellular asymmetry in epithelia. *Fed. Proc.* 41:48–53.
12. Drenckhahn, D., K. Schluter, D. P. Allen, and V. Bennett. 1985. Colocalization of Band 3 with ankyrin and spectrin at the basal membrane of intercalated cells in the rat kidney. *Science (Wash. DC).* 230:1287–1289.
13. Edelman, G. M. 1983. Cell adhesion molecules. *Science (Wash. DC).* 219:450–457.
14. Edelman, G. M. 1984. Modulation of cell adhesion during induction, histogenesis, and perinatal development on the nervous system. *Annu. Rev. Neurosci.* 7:339–377.
15. Ekblom, P. 1981. Determination and differentiation of the nephron. *Med. Biol.* 59:139–160.
16. Farquhar, M. G., and G. E. Palade. 1963. Junctional complexes in various epithelia. *J. Cell Biol.* 17:375–412.
17. Fisher, K. A., and J. Stoeckenius. 1977. Freeze fractured purple membrane particles: protein content. *Science (Wash. DC.).* 197:72–74.
18. Fradet, Y., C. Cordon-Cardo, T. Thompsom, M. E. Daly, W. F. Whitmore, Jr., K. O. Lloyd, M. R. Melamed, and L. L. Old. 1984. Cell surface antigens of human bladder cancer defined by mouse monoclonal antibodies. *Proc. Natl. Acad. Sci. USA.* 81:224–228.
19. Gonzalez-Mariscal, L., B. Chavez de Ramirez, and M. Cereijido. 1985. Tight junction formation in cultured epithelial cells (MDCK). *J. Membr. Biol.* 86:113–125.
20. Goodenough, D. A., and J. P. Revel. 1970. A fine structural analysis of intercellular junctions in the mouse liver. *J. Cell Biol.* 45:272–290.
21. Griffiths, G., K. Simons, G. Warren, and K. T. Tokuyasu. 1983. Immunoelectronmicroscopy using thin, frozen sections: application to studies of the intracellular transport of Semliki forest virus spike glycoproteins. *Methods Enzymol.* 96:435–450.
22. Griffiths, G., G. Warren, P. Quinn, O. Mathieu-Costello, and H. Hoppeler. 1984. Density of newly synthesized plasma membrane proteins in intracellular membranes. I. Stereological studies. *J. Cell Biol.* 98:2133–2141.
23. Gumbiner, B., and K. Simons. 1986. A functional assay for proteins involved in establishing an epithelial occluding barrier: identification of an uvomorulin-like polypeptide. *J. Cell Biol.* 102:457–468.
24. Hall, G. H., D. A. Farson, and M. J. Bissell. 1982. Lumen formation by epithelial cell lines in response to collagen overlay: a morphogenetic model in culture. *Proc. Natl. Acad. Sci. USA.* 79:4672–4676.
25. Herzlinger, D. A., and G. Ojakian. 1984. Studies on the development and maintenance of epithelial cell surface polarity with monoclonal antibodies. *J. Cell Biol.* 98:1777–1787.
26. Hoi Sang, U., M. H. Saier, Jr., and M. H. Ellisman. 1979. Tight junction formation is closely linked to the polar redistribution of intramembranous particles in aggregating MDCK epithelia. *Exp. Cell Res.* 122:384–392.
27. Imhof, B. A., H. P. Vollmers, S. L. Goodman, and W. Birchmeier. 1983. Cell-cell interaction and polarity of epithelial cells: specific perturbation using a monoclonal antibody. *Cell.* 35:667–675.
28. Ingber, D. E., J. A. Madri, and J. D. Jamieson. 1986. Basement membrane as a spatial organizer of polarized epithelia. *Am. J. Pathol.* 122:129–139.
29. Johnson, M. H., and C. A. Ziomek. 1981. Induction of polarity in mouse 8-cell blastomeres: specificity, geometry and stability. *J. Cell Biol.* 91: 303–308.
30. Kohler, G., and C. Milstein. 1975. Continuous culture of fused cells secreting antibody of pre-defined specificity. *Nature (Lond.).* 256:495–497.
31. Lamb, J. F., P. Ogden, and N. L. Simmons. 1981. Autoradiographic localization of [3H] ouabain bound to cultured epithelial cell monolayers of MDCK cells. *Biochim. Biophys. Acta.* 644:333–340.
32. Leighton, J., L. W. Estes, S. Mansukhani, and Z. Brada. 1970. A cell line derived from normal dog kidney (MDCK) exhibiting qualities of papillary adenocarcinoma and of renal tubular epithelium. *Cancer.* 26:1022–1028.
33. Liotta, L. A., C. N. Rao, and S. H. Barsky. 1984. Tumor cell interaction with the extracellular matrix. *In* The Role of the Extracellular Matrix in Development. R. L. Trelstad, editor. Alan R. Liss Inc., New York. 357–372.
34. Louvard, D. 1980. Apical membrane aminopeptidase appears at site of cell-cell contact in cultured kidney epithelial cells. *Proc. Natl. Acad. Sci. USA.* 77:4132–4136.
35. Madin, S. H., and N. B. Darby. 1958. As catalogued. *In* American Type Culture Collection Catalog of Strains. Vol. 2. Rockville, Maryland. 574–576.
36. Matlin, K. S., D. Bainton, M. Pesonen, N. Genty, D. Louvard, and K. Simons. 1983. Transfer of a viral envelope glycoprotein from the apical to the basolateral plasma membrane of MDCK cells. I. Morphological evidence. *J. Cell Biol.* 97:627–637.
37. Matlin, K. S., and K. Simons. 1984. Sorting of an apical plasma membrane glycoprotein occurs before it reaches the cell surface in cultured epithelial cells. *J. Cell Biol.* 99:2131–2139.
38. Michl, J., M. M. Pieczonka, J. C. Unkeless, and S. C. Silverstein. 1979. Effects of immobilized immune complexes on Fc- and complement-receptor function in resident and thioglycollate-elicited mouse peritoneal macrophages. *J. Exp. Med.* 150:607–621.
39. Misek, D. M., E. Bard, and E. J. Rodriguez-Boulan. 1984. Biogenesis of epithelial cell polarity. Intracellular sorting and vectorial exocytosis of an apical plasma membrane protein. *Cell.* 39:537–546.
40. Misfeldt, D. S., S. T. Hamamoto, and D. K. Pitelka. 1976. Transepithelial transport in cell culture. *Proc. Natl. Acad. Sci. USA.* 73:1212–1216.
41. Mooseker, M. S. 1985. Organization, chemistry and assembly of the cytoskeletal apparatus of the intestinal brush border. *Annu. Rev. Cell Biol.* 1:209–241.
42. Moreno, J. H., and J. M. Diamond. 1975. Cation permeation mechanisms and cation selectivity in "tight-junctions" of gallbladder epithelium. *In* Membranes, a Series of Advances. Vol. 3. G. Eisenman, editor. Marcel Dekker, Inc., New York. 383–498.
43. Nelson, W. J., and P. J. Veshnock. 1986. Dynamics of membrane-skeleton (fodrin) organization during development of polarity in Madin-Darby canine kidney epithelial cells. *J. Cell Biol.* 103:1751–1766.
44. Nitsch, L., and S. H. Wollman. 1980. Ultrastructure of intermediate stages in polarity reversal of thyroid epithelium in follicles in suspension culture. *J. Cell Biol.* 86:875–880.
45. Pesonen, M., and K. Simons. 1983. Transepithelial transport of a viral membrane glycoprotein implanted into the apical plasma membrane of Madin-Darby canine kidney cells. II. Immunological quantitation. *J. Cell Biol.* 97:638–643.
46. Pfeiffer, S., S. D. Fuller, and K. Simons. 1985. Intracellular sorting and basolateral appearance of the G protein of vesicular stomatitis virus in Madin-Darby canine kidney cells. *J. Cell Biol.* 101:470–476.
47. Pisam, M., and P. Ripoche. 1976. Redistribution of surface macromolecules in dissociated epithelial cells. *J. Cell Biol.* 71:907–920.
48. Pitelka, D. R., and B. N. Taggart. 1983. Mechanical tension induces lateral movement of intramembrane components of the tight junctions: studies on mouse mammary cells in culture. *J. Cell Biol.* 96:606–612.
49. Pitelka, D. R., B. N. Taggart, and S. T. Hamamoto. 1983. Effects of extracellular calcium depletion on membrane topography and occluding junctions of mammary epithelial cells in culture. *J. Cell Biol.* 96:613–624.
50. Rabito, C. A., and R. Tchao. 1980. [3H] ouabain binding during the monolayer organization and cell cycle in MDCK cells. *Am. J. Physiol.* 238 (*Cell Physiol.* 7):C43-C48.
51. Rindler, M. J., I. E. Ivanov, H. Plesken, and D. D. Sabatini. 1985. Polarized delivery of viral glycoproteins to the apical and basolateral plasma membranes of Madin-Darby canine kidney cells infected with temperature-sensitive viruses. *J. Cell Biol.* 100:136–151.
52. Rodriguez-Boulan, E. 1983. Membrane biogenesis, enveloped RNA viruses, and epithelial polarity. *Mod. Cell Biol.* 1:119–170.
53. Rodriguez-Boulan, E. 1983. Polarized budding of viruses from epithelial cells. *Methods Enzymol.* 98:486–501.
54. Rodriguez-Boulan, E., K. Paskiet, and D. F. Sabatini. 1983. Assembly of enveloped viruses in Madin-Darby canine kidney cells: polarized budding from single attached cells and from clusters of cells in suspension. *J. Cell Biol.* 96:866–874.
55. Rodriguez-Boulan, E., and M. Pendergast. 1980. Polarized distribution of viral envelope proteins in the plasma membrane of infected epithelial cells. *Cell.* 20:45–54.
56. Rodriguez-Boulan, E., and D. D. Sabatini. 1978. Asymmetric budding of viruses in epithelial monolayers: a model system for study of epithelial polarity. *Proc. Natl. Acad. Sci. USA.* 75:5071–5075.
57. Salas, P. J. I., D. E. Misek, D. E. Vega-Salas, D. Gundersen, M. Cereijido, and E. Rodriguez-Boulan. 1986. Microtubules and actin microfilaments are not critically involved in the biogenesis of epithelial cell surface polarity. *J. Cell Biol.* 102:1853–1867.
58. Segrest, J. P., T. Gulik-Krzywicki, and L. Sardet. 1974. Association of the membrane-penetrating polypeptide segment of the human erythrocyte MN-glycoprotein with phospholipid bilayers. I. Formation of freeze-etch intramembranous particles. *Proc. Natl. Acad. Sci. USA.* 71:3294–3297.
59. Simons, K., and S. D. Fuller. 1985. Cell surface polarity in epithelia. *Annu. Rev. Cell Biol.* 1:243–288.
60. Simons, K., and H. Garoff. 1980. The budding mechanisms of enveloped animal viruses. *J. Gen. Virol.* 50:1–21.
61. Sitte, H. 1967. Morphometrische Untersuchungen und Zellen. *In* Quantitative Methods in Morphology. E. R. Wiebel and H. Elias editors. Springer-Verlag, Berlin. 167–198.
62. Smith, Z. D. J., M. J. Caplan, and J. D. Jamieson. 1985. Removal of displaced Na-K ATPase from the apical surface of MDCK cells. *J. Cell Biol.* 101:61a. (Abstr.)
63. Sugrue, S. P., and E. D. Hay. 1981. Response of basal epithelial cell surface and cytoskeleton to solubilized extracellular matrix molecules. *J. Cell Biol.* 91:45–54.
64. Tillack, T. W., R. E. Scott, and V. T. Marchesi. 1972. The structure of erythrocyte membrane studied by freeze-etching. II. Localization of receptors for phytohemagglutinin and influenza virus to the intramembranous particles. *J. Exp. Med.* 135:1209–1227.
65. Towbin, H., T. Staehelin, and J. Gordon. 1979. Electrophoretic transfer

of proteins from polyacrylamide gels to nitrocellulose sheets: procedure and some applications. *Proc. Natl. Acad. Sci. USA.* 76:4350–4354.
66. Tsien, R. Y. 1980. New calcium indicators and buffers with high selectivity against magnesium and protons: design, synthesis and properties of prototype structures. *Biochemistry.* 19:2397–2404.
67. Vega-Salas, D. E., P. J. I. Salas, and E. Rodriguez-Boulan. 1985. Monoclonal antibodies against apical surface antigens of MDCK (epithelial) cells. *J. Cell Biol.* 101:61a. (Abstr.)
67a. Vega-Salas, D. E., P. J. I. Salas, and E. Rodriguez-Boulan. 1987. Modulation of the expression of an apical plasma membrane protein of Madin–Darby Canine Kidney epithelial cells: cell–cell interactions control the appearance of a novel intracellular storage compartment. *J. Cell Biol.* In press.
68. van Meer, G., and K. Simons. 1986. The function of tight junctions in maintaining differences in lipid composition between the apical and the basolateral cell surface domains of MDCK cells. *EMBO (Eur. Mol. Biol. Organ.) J.* 5:1455–1464.
69. von der Mark, K., J. Mollenhauer, U. Kuhl, J. Bee, and H. Lesot. 1984. Anchorins: A new class of membrane proteins involved in cell-matrix interactions. *In* The Role of the Extracellular Matrix in Development. R. L. Trelstad, editor. Alan R. Liss Inc., New York. 67–88.
70. Weibel, E. R. 1969. Stereological principles for morphometry in electron microscopic cytology. *Int. Rev. Cytol.* 26:235–302.
71. Weibel, E. R. 1980. Stereological methods. Vol. 2. Academic Press, Inc., New York. 107–111.
72. White, J., M. Keelian, and A. Helenius. 1983. Membrane fusion proteins of enveloped viruses. *Q. Rev. Biophys.* 16:151–195.
73. Whittembury, G., and F. A. Rawlins. 1971. Evidence of a paracellular pathway for ion flow in the kidney proximal tubule: electron microscopic demonstration of lanthanum precipitate in the tight junction. *Pflugers Arch.* 330:302–309.
74. Yelton, D. E., and M. D. Scharff. 1981. Monoclonal antibodies: a powerful new tool in biology and medicine. *Annu. Rev. Biochem.* 50:657–680.
75. Ziomek, C. A., S. Schulman, and M. Edidin. 1980. Redistribution of membrane proteins in isolated mouse intestinal epithelial cells. *J. Cell Biol.* 86:849–857.